

Nonlinear optical susceptibilities of epitaxially grown polydiacetylene measured by femtosecond time-resolved spectroscopy

Masayuki Yoshizawa

Department of Physics, Faculty of Science, University of Tokyo, Hongo 7-3-1, Bunkyo-ku, Tokyo 113, Japan

Yasuhiro Hattori

New Chemistry R&D Laboratories, Sumitomo Electric Industries, Shimaya 1-1-3 Konohana-ku, Osaka-shi 554, Japan

Takayoshi Kobayashi

Department of Physics, Faculty of Science, University of Tokyo, Hongo 7-3-1, Bunkyo-ku, Tokyo 113, Japan

(Received 23 April 1992; revised manuscript received 26 August 1992)

Ultrafast nonlinear optical responses in polydiacetylene-3-butoxycarbonyl methylurethane prepared by epitaxial vacuum deposition on a KCl substrate are investigated by femtosecond absorption spectroscopy. Absorbance changes due to "instantaneous" processes which decay within the pulse duration of 100 fs, self-trapped exciton, and triplet exciton are resolved in time. The spectra of the corresponding nonlinear optical susceptibilities are obtained considering the pulse duration and response times. The "instantaneous" nonlinear optical response consists of several nonlinear effects, i.e., hole burning, coherent coupling between pump polarization and probe field, Raman gain, inverse Raman scattering, and induced-phase modulation.

I. INTRODUCTION

Conjugated polymers have been extensively investigated both experimentally and theoretically as model compounds of one-dimensional electronic systems. Recently, their large and ultrafast optical nonlinearities have attracted great interest as candidate materials to be applied in nonlinear optical devices.^{1,2} Among many conjugated polymers, polydiacetylenes (PDA's) are most intensively studied because of well-defined sharp excitonic absorption peaks, phase transitions with dramatic color change, and a wide variety of sample forms, i.e., solutions, single crystals, and thin films such as Langmuir-Blodgett films, cast films, spin-coated films, and vacuum-deposited films.³

Nonlinear optical responses in PDA's have been studied by time-resolved nonlinear spectroscopies, i.e., degenerate four-wave mixing,^{4,5} coherent-Raman scattering,⁶ inverse Raman spectroscopy,⁷ optical Kerr effect,^{8,9} the Raman-induced Kerr effect,¹⁰ and absorption saturation.¹¹⁻¹³ However, these works measured only a few wavelengths or near the exciton resonance (1.8–2.2 eV). The nonlinear optical responses in the whole visible and near-infrared region (1.1–3.0 eV) have been investigated by femtosecond pump-probe spectroscopy and several ultrafast nonlinear optical effects, i.e., coherent coupling between pump polarization and probe field, Raman gain, inverse Raman scattering, induced-phase modulation, and perturbed free-induction decay, have been observed.¹⁴⁻¹⁶

Ultrafast relaxation processes of photoexcitations have been investigated in several one-dimensional conjugated polymers, such as PDA's,^{1,2,14-19} polythiophenes (PT's),^{15,16,20,21} and polyacetylenes.²²⁻²⁴ Some PDA's

have several phases with names given according to their color. Blue- and red-phase PDA's have excitonic absorption peaks around 2.0 and 2.3 eV, respectively. Red-phase PDA's have weak fluorescence with the quantum yield of $10^{-(3-4)}$,²⁵ while fluorescence has not been observed in blue-phase PDA's (fluorescence efficiency is therefore estimated to be smaller than 10^{-5}). Yellow-phase solutions of PDA-3KAU (poly [4,6-decadiyn-1,10-diol-bis(carbonyl methylurethane)]) have been studied by picosecond fluorescence spectroscopy and the quantum yield and lifetime of the fluorescence have been obtained as $2.7 \times 10^{-4} - 5.0 \times 10^{-5}$ and 9 ± 3 ps, respectively.¹⁸ Relaxation kinetics in blue- and red-phase PDA's have been investigated by femtosecond absorption spectroscopy.^{1,2,14-17} The ultrafast decay kinetics in both phases have been explained in terms of the geometrical relaxation to form self-trapped excitons (STE's) which decay into the ground state via tunneling in the configuration space. The relaxation processes in PT's can be explained using the same model with PDA's.^{15,16,20}

In this paper, the ultrafast nonlinear optical response and relaxation kinetics in blue-phase PDA-3BCMU (3-butoxycarbonyl methylurethane) epitaxially grown on a KCl substrate have been investigated by femtosecond absorption spectroscopy. The transient absorbance changes are time-resolved in the wide spectral region extending from 1.2 to 2.8 eV. The spectral changes were attributed to four components with different time responses. They are "instantaneous" processes, free excitons, STE's, and triplet excitons. The corresponding nonlinear optical susceptibilities of these components are estimated considering the pulse duration and response times of the nonlinear processes. The spectrum of the "instantaneous" response can be explained by a model including the cou-

pling between excitons and vibrational modes. Several nonlinear optical effects, such as hole burning, coherent coupling, and Raman processes, are observed. The relaxation processes of photogenerated excitons in epitaxially grown PDA-3BCMU are compared with those in PDA-3BCMU cast film.

II. EXPERIMENT

The femtosecond absorption spectroscopy system consists of a colliding-pulse mode-locked dye laser, a four-stage dye amplifier pumped by the second-harmonic pulses of a 10-Hz *Q*-switched Nd:YAG (yttrium aluminum garnet) laser, and an optical system for pump-probe absorption spectroscopy.¹⁴ The center wavelength and duration of the amplified pulses are 628 nm (1.97 eV) and about 100 fs, respectively. The amplified pulses were split into two beams for pump and probe spectroscopy. The excitation photon density used in this study is 1.7×10^{15} photons/cm². The probe white continuum was generated by self-phase modulation in a 1-mm CCl₄ cell. Since the white continuum has a strong sharp peak at the laser wavelength, a thin blue color filter was used to decrease the intensity around 630 nm. The spectrum of the probe pulse is shown below in Fig. 3. The total photon density of the probe pulse at a sample is about 1×10^{14} photons/cm². The chirp of the white continuum and the time resolution were measured by the cross-correlation method using sum-frequency generation of pump and probe pulses. The full width at half maximum (FWHM) of the cross-correlation curves is between about 140 and 250 fs depending on the probe wavelength. The experiment was performed using a continuous-gas-flow cryostat (Oxford, CF104), which kept the samples of polydiacetylene under vacuum and at a temperature between 10 and 290 K.

PDA-3BCMU (3-butoxycarbonylmethylurethane) has side groups of



in the backbone chain structure of $(=RC-C\equiv C-CR'=)_n$. PDA-3BCMU is one of the well-known soluble PDA's. A PDA-3BCMU thin film prepared by the casting method has been investigated by femtosecond spectroscopy.^{14,15} In this study, the diacetylene monomers were epitaxially grown on a KCl[001] surface and polymerized using UV light.²⁶ A single crystal of KCl was cleaved in air and heated at 150°C for 30 min in a vacuum chamber before deposition. The deposition rate of the monomer was controlled at 0.3 nm/min under the pressure of 3×10^{-5} Torr. The substrate was kept at 45°C during the deposition. The monomer crystals grown on the KCl surface have a square shape of 2×2 μm. From an analysis of the electron-diffraction pattern, the crystals were bioriented and monomer molecules were perpendicular to the substrate surface stacking along the KCl[110] or $[1\bar{1}0]$ direction. The thickness of the crystal was 0.1–0.5 μm. The monomer crystals were irradiated by UV light (254 nm) to polymerize. The polymerized sample is a blue-phase PDA and has an excitonic absorption peak at 1.97 eV, as shown in Fig. 1. The backbone chains of polymerized crystals in the area of

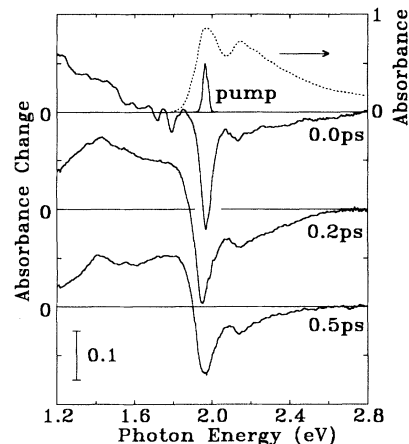


FIG. 1. Transient absorption spectra of blue-phase PDA-3BCMU on a KCl substrate at 290 K. The stationary absorption (dotted curve) and pump spectra are shown together.

about 1×1 mm align to one of the directions ($[110]$ and $[1\bar{1}0]$) of the KCl crystal. The dichroic ratio of the absorption peak at 1.97 eV is about 5.

III. RELAXATION KINETICS OF EXCITONS

The photoinduced absorption spectra of a PDA-3BCMU film of 0.13-μm thickness at 290 K are shown in Fig. 1, together with the stationary absorption and pump spectra. Both polarizations of the pump and probe light are parallel to the orientational direction of the polymer chain. The structure and kinetics of the transient absorbance change in the epitaxially grown PDA-3BCMU are very similar to those observed in other PDA's, i.e., cast films of PDA-3BCMU, vacuum-deposited films of PDA-4BCMU (4-butoxycarbonyl methylurethane), and PDA-(12,8) (poly[pentacos-10,12-diyonic acid]) LB films.^{14–17} A sharp bleaching peak at 1.97 eV is due to saturation of the excitonic absorption and coherent coupling between pump polarization and probe field. Two negative peaks at 1.79 and 1.71 eV are observed at the delay time of 0.0 ps. They are due to the Raman gain of the stretching vibrations of the C=C and C≡C bonds, respectively.

At 0.0 ps, the photoinduced absorbance change below 1.8 eV is larger at lower probe photon energies down to 1.2 eV. Then the absorption shifts to higher energies with time from 0.0 to 0.5 ps and has two peaks at 1.8 and 1.4 eV. This spectral change is explained by the geometrical relaxation of free excitons to self-trapped excitons (STE's).^{14–17} The photoexcited free excitons are coupled with the C—C stretching modes within the phonon periods of 10–20 fs and become nonthermal STE's. Then the nonthermal STE's thermalize and relax to the bottom of their potential surfaces. Therefore, the transient absorption is shifted to higher energy. The absorption peak at 1.8 eV is assigned to the transitions from the lowest 1B_u exciton to a biexciton with 1A_g symmetry and the peak at 1.4 eV is assigned to the transition from the 1B_u exciton to a higher 1A_g exciton.¹⁷

Figure 2 shows the time dependence of the absorbance changes. The bleaching at 1.95 eV appears just after pho-

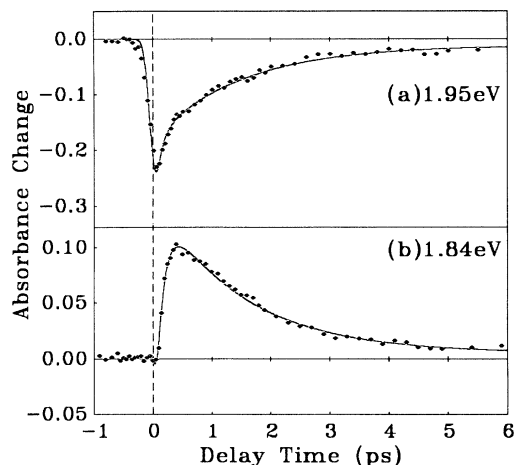


FIG. 2. Time dependence of absorbance changes at (a) 1.95 eV and (b) 1.84 eV. Solid curves are the best fit of Eqs. (2) and (1) to the data at 1.95 and 1.84 eV, respectively. The time constants τ_f and τ_s are (a) 150 fs and 1.4 ps and (b) 150 fs and 1.5 ps, respectively. The resolution times at 1.95 and 1.84 eV are obtained by a cross-correlation method as 200 and 150 fs, respectively.

toexcitation, while the absorbance change at 1.84 eV increases slower than the resolution time. The transient response at 1.84 eV can be fitted to

$$\Delta A(t) = \Delta A_s \{ \exp(-t/\tau_s) - \exp(-t/\tau_f) \} + \Delta A_c, \quad (1)$$

where τ_f and τ_s are rise and decay time constants and ΔA_c is a long-lived component due to triplet excitons. The resolution time at 1.84 eV is obtained as 150 fs by the cross-correlation method and convoluted to Eq. (1) using a Gaussian function. The rise time τ_f corresponds to the time constant of the spectral change due to the thermalization of nonthermal STE's and is obtained as 150 ± 40 fs.

In the red-phase PDA-4BCMU, another slower spectral change with the time constant of 1.1 ± 0.1 ps has been observed.¹⁶ The fast spectral change is assigned to relaxation from nonthermal STE's to quasithermal STE's among the vibrational modes within a single chain of the polymer. The slow spectral change in the red-phase PDA is assigned to relaxation from quasithermal STE's to thermal STE's associated with energy distribution induced by the coupling between the intrachain and inter-chain vibrational modes. These fast and slow processes were referred to in previous papers as the relaxation from unrelaxed STE's to unthermalized STE's by phonon emission, and the thermalization from unthermalized STE's to thermalized STE's, respectively.^{1,2,16,17} Relaxation kinetics in molecular systems have similar two-step thermalization processes called intramolecular and intermolecular vibrational relaxations.²⁷ However, the spectral change due to the relaxation from the quasithermal STE's to the thermal STE's could not be observed in the blue-phase PDA. The decay time constant τ_s corresponds to the relaxation-time constant from the quasithermal STE's to the ground state and is obtained as $\tau_s = 1.5 \pm 0.1$ ps at 1.84 eV.

The signals due to nonthermal STE's and "instantaneous" nonlinear effects such as coherent coupling and Raman gain are expected to be contained in the absorbance change at 1.95 eV. Therefore, the time dependence at 1.95 eV is fitted to

$$\Delta A(t) = \Delta A_0 \delta(t) + \Delta A_f \exp(-t/\tau_f) + \Delta A_s \{ \exp(-t/\tau_s) - \exp(-t/\tau_f) \} + \Delta A_c, \quad (2)$$

where the first term is the term which responds within the pulse duration and ΔA_f corresponds to the absorbance change due to nonthermal STE's. When the time constant τ_f is fixed to 150 fs, the time constant τ_s is obtained as 1.4 ± 0.1 ps. This is consistent with the decay-time constant obtained at 1.84 eV. However, when the change in the transient absorption spectra due to thermalization takes place, the overall decrease in the absorbance change due to depopulation of STE's also takes place. Therefore, the time constants determined at other photon energies are slightly different from those at 1.84 and 1.95 eV. The decay kinetics at 10 K are similar to those at 290 K and the time constants are estimated as $\tau_f = 130 \pm 40$ fs and $\tau_s = 2.0 \pm 0.2$ ps, using the time dependence of the absorbance change at 1.82 eV.

The decay kinetics in the epitaxially grown PDA-3BCMU has the same time constants as the cast film of PDA-3BCMU.¹⁵ All blue-phase PDA's investigated by femtosecond spectroscopy show similar time-resolved spectral changes with similar decay kinetics giving approximately the same time constants, $\tau_f = 150$ fs and $\tau_s = 1.5$ ps at 290 K, and $\tau_f = 150$ fs and $\tau_s = 2.0$ ps at 10 K.¹⁴⁻¹⁷ Therefore, it can be concluded that the relaxation processes of the photogenerated excitons in blue-phase PDA's in the femtosecond to 10-ps time region are very insensitive to the sample morphology and the side groups. This strongly supports the argument that the observed spectral changes in this time region are due to intrinsic processes, such as the free-exciton self-trapping associated with geometrical relaxation, thermalization, and tunneling from the STE to the ground state. These processes are little affected by the structural defects or impurities, even though their concentrations may be moderately high in disordered systems such as cast films.

IV. NONLINEAR OPTICAL SUSCEPTIBILITIES MEASURED BY TIME-RESOLVED SPECTROSCOPY

The third-order nonlinear optical susceptibilities have been measured by various methods, i.e., third-harmonic generation, degenerate four-wave mixing, optical Kerr effect, and absorption saturation. In this study, the nonlinear optical susceptibility is investigated by femtosecond time-resolved absorption spectroscopy. The optical susceptibility χ is defined in the cgs unit system by

$$P = \chi^{(1)}E + \chi^{(2)}EE + \chi^{(3)}EEE + \cdots + \chi^{(n)}E^n + \cdots, \quad (3)$$

where P and E are the polarization and the electric field, respectively, and $\chi^{(n)}$ are the n th-order nonlinear suscep-

tibilities. The spectrum of the imaginary part of the third-order nonlinear susceptibility, $\text{Im}[\chi^{(3)}(-\omega_2; \omega_2, -\omega_1, \omega_1)]$, can be obtained by pump-probe absorption spectroscopy, where ω_1 and ω_2 are the frequencies of the pump and probe lights, respectively. Higher-order nonlinear susceptibilities can also be obtained if the time-resolved difference spectrum is dependent on the pump intensity.

When the nonlinear optical susceptibility is to be determined by time-resolved spectroscopy, the value is usually evaluated using the peak intensity of the pulse. In this case, experiments using the same nonlinear optical system with different pump durations give different values of nonlinear susceptibilities. For example, the nonlinear susceptibilities observed by pulses with the duration much shorter than the response time is smaller than those obtained by longer pulses, because the signal is proportional not to the peak intensity but to the pulse energy, and shorter pulses give higher peak intensities for the

same pulse energy. Therefore, the resolution time of the experiments should be considered in the calculation of the nonlinear susceptibilities.

The observed transient responses in the PDA-3BCMU are resolved in times using Eq. (2). The δ -function term is due to "instantaneous" nonlinear effects which decay within the pulse duration of 100 fs. ΔA_f and ΔA_s correspond to the absorbance changes due to the nonthermal STE and the quasithermal STE, respectively. The time constants are $\tau_f = 150$ fs and $\tau_s = 1.5$ ps at 290 K. The long-lived component ΔA_c is due to triplet excitons. The lifetime of the triplet excitons has been obtained as 44 μ s in PDA-TS (polydiacetylene-*p*-toluene sulfonate) and is much longer than the time constants of the STE's.²⁸

The nonlinear optical susceptibility of the transient response with the lifetime τ is estimated as follows. When excitation with the lifetime τ is induced by an excitation pulse $I_{\text{ex}}(t)$ and probed by a probe pulse $I_{\text{pr}}(t)$, the observed absorbance change $\Delta A(t)$ is given by

$$\Delta A(t) = \frac{\int_{-\infty}^{\infty} dt'' I_{\text{pr}}(t''-t) \int_{-\infty}^{t''} dt' a I_{\text{ex}}(t') \exp[-(t''-t')/\tau]}{\int_{-\infty}^{\infty} dt'' I_{\text{pr}}(t'')}, \quad (4)$$

where a is a constant which is proportional to the imaginary part of the third-order nonlinear susceptibility.

The absorbance change observed by continuous excitation and probe light is obtained from Eq. (4) as

$$\Delta A_{\text{cw}} = a I_{\text{ex}} \tau. \quad (5)$$

In this case, the third-order nonlinear susceptibility measured by the pump-probe spectroscopy is defined as

$$\text{Im}[\chi^{(3)}(-\omega_2; \omega_2, -\omega_1, \omega_1)] = \frac{2.303 \Delta A_{\text{cw}} n(\omega_1) n(\omega_2) c^2}{192 \pi^2 \omega_2 I_{\text{ex}} L}, \quad (6)$$

where $n(\omega_1)$ and $n(\omega_2)$ are the real refractive indices at the frequencies of ω_1 and ω_2 , respectively, c is the velocity of light in vacuum, and L is the thickness of a sample.

When the lifetime τ is much shorter than the pulse duration t_p , the observed absorbance change at time zero $\Delta A(0)$ is equal to ΔA_{cw} , and the nonlinear susceptibility can be calculated using Eq. (6). When the duration of the pump and probe pulses is nearly equal to or shorter than the lifetime ($t_p \lesssim \tau$), the absorbance change at time zero is different from ΔA_{cw} . Assuming that the excitation and probe pulse shapes are rectangular with duration t_p , the observed absorbance change at delay-time zero is obtained as

$$\Delta A(0) = a I_{\text{ex}} \tau \{1 + [\exp(-t_p/\tau) - 1] \tau / t_p\}. \quad (7)$$

Even if the pulse shape is different from the rectangular shape, the calculated result does not change much, since the pulse has a sech^2 shape. The absorbance change for a delay time longer than the pulse duration ($t > t_p$) is given by

$$\Delta A(t) = \Delta A_i \exp(-t/\tau) = \frac{4a I_{\text{ex}} \tau^2}{t_p} \sinh^2(t_p/2\tau) \exp(-t/\tau). \quad (8)$$

Then the response for the continuous excitation and probe ΔA_{cw} can be obtained from Eqs. (5) and (8) as a

$$\Delta A_{\text{cw}} = \frac{\Delta A_i t_p}{4\tau \sinh^2(t_p/2\tau)}. \quad (9)$$

Equation (9) can be simplified for $t_p \ll \tau$ as

$$\Delta A_{\text{cw}} = \Delta A_i \tau / t_p. \quad (10)$$

The nonlinear susceptibility measured by the pulses with the duration t_p can be estimated using Eqs. (6) and (9). The third-order nonlinear optical properties of materials with response time τ are often evaluated by a figure of merit $F_m = \chi^{(3)}/\alpha\tau$, where α is the absorption coefficient at the laser wavelength. The figure of merit can be defined only when the response time and the absorption coefficient are finite. In this study, the nonlinear optical properties are investigated in the wide region from 1.2 to 2.8 eV, considering the pulse duration and response times.

The photoinduced absorbance change ΔA is usually proportional to the imaginary part of the nonlinear optical susceptibility as given by Eq. (6). However, the wavelength of the probe light is shifted by the change of the refractive index n . The shift is proportional to the time derivative as

$$\Delta\omega = \frac{\omega L}{c} \frac{dn}{dt}. \quad (11)$$

Then the derivative of the probe spectrum appears in the

observed absorbance change as

$$\Delta A(\omega) = -\frac{\omega L}{2.303cI_{\text{pr}}} \frac{dI_{\text{pr}}}{d\omega} \frac{dn}{dt}. \quad (12)$$

The transient transmission change due to induced-phase modulation (IPM) observed in femtosecond spectroscopy of several materials such as red-phase PDA-4BCMU (Ref. 16) must be corrected. The transmission change due to IPM is observed even when there is no real absorbance change in some spectral region. The artificial absorbance change has been observed in CS₂ liquid.²⁹ Care must be taken to obtain the real absorbance change spectrum to eliminate the effects of IPM, coherent artifact (CA), and perturbed free-induction decay (PFID).³⁰

Figure 3 shows the signal due to IPM expected to be observed in this study. The white continuum generated from the 1.97-eV pulse has a peak around 2 eV. After passing through a thin blue color filter the probe spectrum has two peaks at 1.97 and 1.75 eV. The refractive index change spectrum Δn shown in Fig. 3 is calculated from the absorbance change at 0.2 ps using the Kramers-Kronig (KK) relations. The application of the KK relation to obtain the refractive index is useful only when the transmittance changes due to IPM, CA, and PFID are much smaller than the real absorbance change. This condition is found to be satisfied, as discussed below. Then the expected signals due to IPM at 0.0 ps are calculated using Eq. (12). Since the change of the refractive index due to photogenerated excitons is negative around 1.9 eV, the probe pulse shifts to a higher frequency and the observed absorbance change has a positive peak at 1.92 eV. The oscillatory structure comes from the structure of the probe spectrum. The maximum signal due to IPM is expected to be 0.006 and is much smaller than the observed absorbance change in this study. Since the time derivative of the refractive index has a maximum value at 0.0 ps and becomes smaller at the longer delay time, the transmittance changes due to IPM can be neglected in the ΔA_f , ΔA_s , and ΔA_c spectra shown below.

V. NONLINEAR OPTICAL RESPONSES DUE TO EXCITONS

The imaginary part of the nonlinear susceptibility due to the "instantaneous" processes is estimated and shown

$$\chi_{00'}^{(3)} = \frac{|\mu_{00'}|^4}{\hbar^3} \left\{ \frac{4\Gamma_x/\gamma_x}{[(\omega_1 - \omega_x)^2 + \Gamma_x^2](\omega_2 - \omega_x + i\Gamma_x)} \right. \quad (13a)$$

$$+ \frac{2}{(\omega_1 - \omega_x - i\Gamma_x)(\omega_2 - \omega_x + i\Gamma_x)(\omega_2 - \omega_1 + i\gamma_x)} \quad (13b)$$

$$\left. - \frac{2}{(\omega_2 - \omega_x + i\Gamma_x)^2(\omega_2 - \omega_1 + i\gamma_x)} \right\}, \quad (13c)$$

where ω_1 and ω_2 are the frequencies of the pump and probe fields, respectively, and $\mu_{00'}$, ω_x , Γ_x , and γ_x are the dipole moment, the transition frequency, the transverse relaxation rate, and the longitudinal relaxation rate of the exciton, respectively.

$\chi^{(3)}$, corresponding to the 1-0' transition, is calculated using a three-level model as

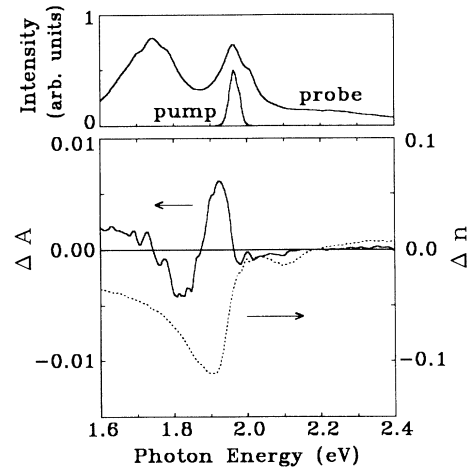


FIG. 3. Photoinduced refractive index change Δn (dotted curve) and calculated absorbance change signal ΔA due to the induced-phase modulation (solid curve). Pump and probe spectra are shown in the upper part.

in Fig. 4(d). Here, the transmittance change due to IPM is corrected in the ΔA_0 spectrum. The spectrum has two negative minima at 1.71 and 1.79 eV, and small dispersion-type structures at 2.15 and 2.23 eV. These structures can be explained by calculating $\chi^{(3)}$ using a model shown in Fig. 4(d). Here, zero-phonon ($\nu=0$) and one-phonon ($\nu=1$) states of four major vibrational modes³¹ are taken into consideration in both the exciton (S_1) and ground levels (S_0). Since the spectral bandwidth of the pump pulse (0.03 eV) is much smaller than the phonon energies (0.11–0.26 eV) and the 1.97-eV pump pulse (ω_1) is resonant with the 0-0' and 1-1' transitions, the pump resonances with the 0-1' and 1-0' transitions are neglected. The nonlinear susceptibilities of three probe resonant transitions (0-0', 1-0', and 0-1') are calculated using the two- and three-level density-matrix models of Dick and Hochstrasser.^{32,33}

$\chi^{(3)}$, corresponding to the 0-0' exciton transitions, is calculated using a two-level model and given by

$$\chi_{10'}^{(3)} = \frac{|\mu_{00'}|^2 |\mu_{10'}|^2}{\hbar^3} \left\{ \frac{2\Gamma_x / \gamma_x}{[(\omega_1 - \omega_x)^2 + \Gamma_x^2](\omega_2 - \omega_x + \omega_i + i\Gamma_x)} \right. \quad (14a)$$

$$\left. + \frac{1}{(\omega_1 - \omega_x - i\Gamma_x)(\omega_2 - \omega_x + \omega_i + i\Gamma_x)(\omega_2 - \omega_1 + \omega_i + i\Gamma_i)} \right\}, \quad (14b)$$

where $\mu_{10'}$ is the dipole moment of the 1-0' transition and ω_i and Γ_i^{-1} are the frequency and the decay rate of each phonon mode, respectively.

Since the pump pulse is resonant with both the 0-0' and 1-1' transition, the nonlinear susceptibility for the 0-1' transition is rather complicated and obtained as

$$\chi_{01'}^{(3)} = \frac{|\mu_{00'}|^2 |\mu_{01'}|^2}{\hbar^3} \left\{ \frac{2\Gamma_x / \gamma_x}{[(\omega_1 - \omega_x)^2 + \Gamma_x^2](\omega_2 - \omega_x - \omega_i + i\Gamma_x)} \right. \quad (15a)$$

$$\left. + \frac{1}{(\omega_1 - \omega_x - i\Gamma_x)(\omega_2 - \omega_x - \omega_i + i\Gamma_x)(\omega_2 - \omega_1 - \omega_i + i\Gamma_i)} \right. \quad (15b)$$

$$\left. - \frac{1}{(\omega_2 - \omega_x - \omega_i + i\Gamma_x)^2(\omega_2 - \omega_1 - \omega_i + i\Gamma_x)} \right\} \quad (15c)$$

$$- \frac{|\mu_{11'}|^2 |\mu_{01'}|^2}{\hbar^3} \frac{1}{(\omega_2 - \omega_x - \omega_i + i\Gamma_x)^2(\omega_2 - \omega_1 - \omega_i + i\Gamma_x)}, \quad (15d)$$

where $\mu_{11'}$ and $\mu_{01'}$ are the dipole moments of the 1-1' and 0-1' transitions, respectively. The common level of the transition in terms (15a)–(15c) is the ground level (S_{00}), while the common level of term (15d) is the excited level ($S_{11'}$).

The imaginary parts of each term and the total of the calculated nonlinear susceptibilities are shown in Fig. 4 with the observed spectrum. Here, the phonon energies of the C=C and C≡C stretching vibrational modes are determined from the observed Raman gain signal as 0.180 and 0.257 eV, respectively. The observed pump spectrum is also used for the calculation. The reported values of the PDA-TS are used for the energies of the other two vibrational modes, the cross sections of each

transition, and $\Gamma_i = 0.003$ eV.³¹ The relaxation rates Γ_x and γ_x and the width of the inhomogeneous broadening are used as variable parameters to fit both the third-order nonlinear susceptibility and the stationary absorption spectra. Then the calculation with $\Gamma_x = 0.03$ eV and $\gamma_x = 0.03$ eV gives a good fit, as shown in Fig. 4(d).

Terms (13a), (14a), and (15a), of which spectra are shown in Fig. 4(a), correspond to the level population term of the transient transmittance change calculated using a two-level system.³⁰ The three terms are hole burning, hot luminescence, and hole burning of phonon sidebands, respectively. Terms (13b), (14b), and (15b) correspond to the pump polarization coupling terms.³⁰ Term (13b) is due to the coherent coupling between pump po-

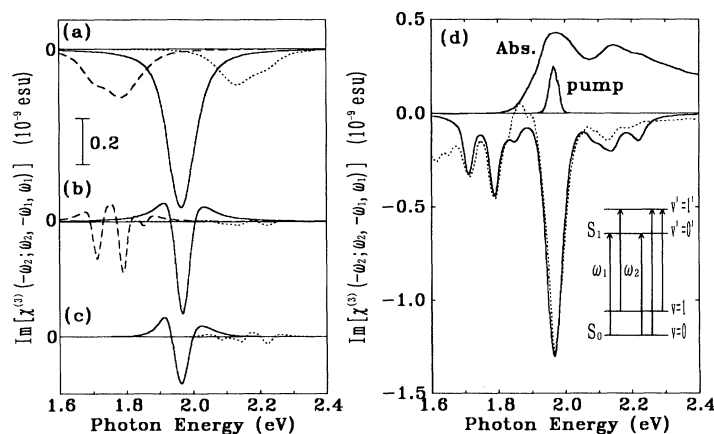


FIG. 4. The third-order nonlinear susceptibilities calculated using the inset model. (a) Level population terms, Eq. (13a) (solid curve), Eq. (14a) (dashed curve), and Eq. (15a) (dotted curve). (b) Pump polarization coupling terms, Eq. (13b) (solid curve), Eq. (14b) (dashed curve), and Eq. (15b) (dotted curve). (c) Perturbed free induction decay terms, Eq. (13c) (solid curve), and Eqs. (15c) + (15d) (dotted curve). (d) Total of the calculated nonlinear susceptibilities (solid curve) and the observed nonlinear susceptibility of the “instantaneous” processes (dotted curve). The stationary absorption and pump spectra are shown together.

larization and probe field. Terms (14b) and (15b) are the stimulated Raman signals in the Stokes (Raman gain) and anti-Stokes sides, respectively. Terms (13c) and (15c) correspond to the perturbed free-induction-decay term.³⁰ The last term (15d) is the inverse Raman scattering.³⁴

The peaks due to Raman gain at 1.71 and 1.79 eV are clearly reproduced in the calculated nonlinear susceptibility. The small peaks at 2.14 and 2.22 eV are due both to the phonon sideband hole and to inverse Raman scattering. When the pump pulse is nearly resonant to the exciton transition, the inverse Raman signal has a dispersive structure.³⁴ The inverse Raman signal in this study is diminished by inhomogeneous broadening of the exciton transition and the broad pump spectrum because of the overlapping of the dispersive structure. The calculated spectrum differs slightly from the observed spectrum around 1.6 and 1.85 eV. It is mainly due to the deviation of the decay kinetics from the biexponential function given by Eq. (2). The relaxation from the nonthermal STE to the quasithermal STE has the time constant of 150 fs, but the transient absorbance change due to the spectral shift cannot be exactly fitted to the exponential function. Therefore, the small deviations appear in the time-resolved spectrum.

The imaginary part of the third-order nonlinear susceptibility spectra $\text{Im}[\chi_{1111}^{(3)}(-\omega_2; \omega_2, -\omega_1, \omega_1)]$ is also estimated from ΔA_f and ΔA_s spectra using Eqs. (6) and (9). The nonlinear susceptibility $\text{Im}[\chi_f^{(3)}]$ shown in Fig. 5(a) is due to the nonthermal STE with the decay time of 150 fs. The spectrum has a negative peak at 1.93 eV and is positive below 1.8 eV. $\text{Im}[\chi_s^{(3)}]$ in Fig. 5(b) is due to the quasithermal STE. The decay time of $\chi_s^{(3)}$ is 1.5 ps. The spectrum has a positive peak at 1.82 eV and a negative peak at 1.96 eV. The peak value of $\text{Im}[\chi_s^{(3)}]$ is 1.0×10^{-8} esu. It is larger than $\text{Im}[\chi_f^{(3)}]$ because the decay time of the quasithermal STE is ten times longer than that of the nonthermal STE. The nonlinear susceptibility

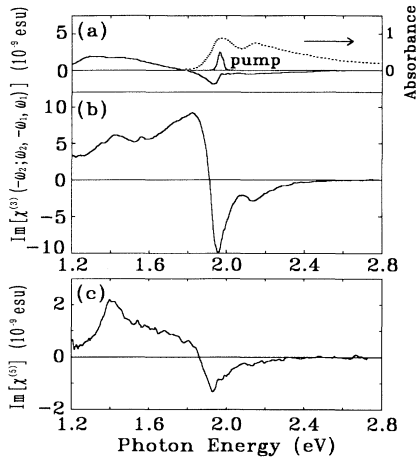


FIG. 5. The third-order nonlinear susceptibilities due to (a) nonthermal self-trapped excitons, (b) quasithermal self-trapped excitons, and (c) the fifth-order nonlinear susceptibility due to triplet excitons. The stationary absorbance and pump spectra are shown together.

of the PDA-3BCMU epitaxially grown on KCl is larger than that of the PDA-3BCMU cast film,¹⁵ because the main chains of the polymers align to the polarization of the pump and probe beams and the inhomogeneous broadening is narrower.

Figure 5(c) shows the nonlinear susceptibility spectrum $\text{Im}[\chi_{TE}^{(5)}]$ due to the triplet exciton. The $\text{Im}[\chi_{TE}^{(5)}]$ has a positive peak at 1.42 eV and a negative peak at 1.94 eV. Since the triplet excitons are generated by the fusion of two singlet excitons,^{1,35} ΔA_c increases proportionally as the square of the pump intensity. Therefore, the observed response corresponds to the fifth-order nonlinearity. Here, the lifetime of the triplet exciton is assumed to be 44 μs using the reported lifetime in the PDA-TS.²⁸ If pump pulses of 1-ps duration and 100-GHz repetition rate (10-ps interval) are used for excitation, the pulses with the peak intensity of about 300 kW/cm^2 give the same amount of signal due to triplet excitons as the ultrafast nonlinear optical responses due to free excitons and STE's. Since slow nonlinear optical effects prevent the ultrafast responses, attention must be paid to their properties for applications in devices at a high repetition rate.

VI. CONCLUSION

The ultrafast nonlinear optical responses in the blue-phase PDA-3BCMU epitaxially grown on a KCl substrate have been investigated. The relaxation kinetics of the photoexcitations can be explained in terms of a STE using the same model as other conjugated polymers.¹⁶ The relaxation processes have the same time constants as a PDA-3BCMU cast film and other blue-phase PDA's. The relaxation processes of excitons in PDA's in the femtosecond to picosecond time range up to 10 ps are insensitive to the sample morphology and the side groups. This indicates that the ultrafast relaxation process in PDA's is due to intrinsic processes, such as self-trapping, thermalization, and tunneling, which are not much affected by structural defects or impurities.

The ultrafast nonlinear optical responses of the PDA-3BCMU are time resolved and separated into four components, including an "instantaneous" nonlinear response term which decays within 100 fs, a nonthermal STE, a quasithermal STE, and a triplet exciton. The spectra of the nonlinear optical susceptibilities are determined taking into account the pulse duration and response times. The spectrum of the "instantaneous" nonlinear optical response is explained using a model of the two-level system with vibrational modes coupled to the excitonic transition. The "instantaneous" nonlinear response consists of several nonlinear effects, i.e., hole burning, coherent coupling between pump polarization and probe field, Raman gain, hole burning of phonon sidebands, and inverse Raman scattering. The contribution of the induced-phase modulation to the observed absorbance change is also estimated.

The nonlinear optical effects due to the nonthermal and quasithermal STE's are the saturation of the excitonic absorption and the transition from the photoexcited lowest 1B_u exciton to a biexciton and/or a higher exciton

with 1A_g symmetry. The decay times of the nonlinear processes due to nonthermal and quasithermal STE's are 150 fs and 1.5 ps at 290 K, respectively. The imaginary part of $\chi^{(3)}(-\omega_2; \omega_2, -\omega_1, \omega_1)$ due to the quasithermal STE has a peak minimum of -1.0×10^{-8} esu at $\hbar\omega_1 = 1.97$ eV and $\hbar\omega_2 = 1.95$ eV.

ACKNOWLEDGMENTS

This research was partly supported by a research grant from the Kurata Foundation and a grant from the Itoh Science Foundation to M.Y. and T.K. and a grant from the Toray Science Foundation to T.K.

- ¹T. Kobayashi, in *Polymers for Lightwave and Integrated Optics*, edited by L. A. Hornak (Dekker, New York, 1992), pp. 543–594.
- ²T. Kobayashi, IEICE Trans. Fundamentals **E-75A**, 38 (1992).
- ³See, e.g., *Polydiacetylenes*, edited by D. Bloor and R. R. Chance (Nijhoff, Dordrecht, 1985).
- ⁴G. M. Carter, J. V. Hryniewicz, M. K. Thakur, Y. J. Chen, and S. E. Meyler, Appl. Phys. Lett. **49**, 998 (1986).
- ⁵T. Hattori and T. Kobayashi, Chem. Phys. Lett. **133**, 230 (1987).
- ⁶J. Swiatkiewicz, X. Mi, P. Chopra, and P. N. Prasad, J. Chem. Phys. **87**, 1882 (1987).
- ⁷G. J. Blanchard and J. P. Heritage, J. Chem. Phys. **93**, 4377 (1990).
- ⁸P. P. Ho, N. L. Yang, T. Jimbo, Q. Z. Wang, and R. R. Alfano, J. Opt. Soc. Am. B **4**, 1025 (1987).
- ⁹F. Charra and J. M. Nunzi, in *Organic Molecules for Nonlinear Optics and Photonics*, edited by J. Messier et al. (Kluwer, Dordrecht, 1991), pp. 359–368.
- ¹⁰T. Kobayashi and M. Yoshizawa, Synth. Met. **41-43**, 3129 (1991).
- ¹¹F. Kajzar, L. Rothberg, S. Etamad, P. A. Chollet, D. Grec, A. Boudet, and T. Jedju, Opt. Commun. **66**, 55 (1988).
- ¹²M. Sinclair, D. McBranch, D. Moses, and A. J. Heeger, Appl. Phys. Lett. **53**, 2374 (1988).
- ¹³B. I. Greene, J. Orenstein, and S. Schmitt-Rink, Science **247**, 679 (1990).
- ¹⁴M. Yoshizawa, M. Taiji, and T. Kobayashi, IEEE J. Quantum Electron. **QE-25**, 2532 (1989).
- ¹⁵T. Kobayashi, M. Yoshizawa, U. Stamm, M. Taiji, and M. Hasegawa, J. Opt. Soc. Am. B **7**, 1558 (1990).
- ¹⁶M. Yoshizawa, A. Yasuda, and T. Kobayashi, Appl. Phys. B **53**, 296 (1991).
- ¹⁷M. Yoshizawa and T. Kobayashi, in *Ultrafast Processes in Spectroscopy 1991*, edited by A. Laubereau and A. Seilmeier (Institute of Physics, Bristol, 1992), pp. 503–508.
- ¹⁸S. Koshihara, T. Kobayashi, H. Uchiki, T. Kotaka, and H. Ohnuma, Chem. Phys. Lett. **114**, 446 (1985).
- ¹⁹J. M. Huxley, P. Mataloni, R. W. Schoenlein, J. G. Fujimoto, E. P. Ippen, and G. M. Carter, Appl. Phys. Lett. **56**, 1600 (1990).
- ²⁰U. Stamm, M. Taiji, M. Yoshizawa, T. Kobayashi, and K. Yoshino, Mol. Cryst. Liq. Cryst. **182A**, 147 (1990).
- ²¹I. D. W. Samuel, K. E. Meyer, S. C. Graham, R. H. Friend, J. Rühle, and G. Wegner, Phys. Rev. B **44**, 9731 (1991).
- ²²C. V. Shank, R. Yen, R. L. Fork, J. Orenstein, and G. L. Baker, Phys. Rev. Lett. **49**, 1660 (1982).
- ²³L. Rothberg, T. M. Jedju, S. Etamad, and G. L. Baker, IEEE J. Quantum Electron. **QE-24**, 311 (1988).
- ²⁴M. Yoshizawa, T. Kobayashi, K. Akagi, and H. Shirakawa, Phys. Rev. B **37**, 10301 (1988).
- ²⁵K. S. Wong, W. Hayes, T. Hattori, R. A. Taylor, J. F. Ryan, K. Kaneto, K. Yoshino, and D. Bloor, J. Phys. C **18**, L843 (1985).
- ²⁶Y. Hattori, A. Mizoguchi, Y. Ogaki, and A. Nishimura (unpublished).
- ²⁷*Radiationless Processes in Molecules and Condensed Phases*, edited by F. K. Fong (Springer-Verlag, Berlin, 1976).
- ²⁸T. Kobayashi and H. Ikeda, Chem. Phys. Lett. **133**, 54 (1987).
- ²⁹E. Tokunaga, A. Terasaki, K. Tsunetomo, Y. Osaka, and T. Kobayashi, Phys. Rev. B (to be published).
- ³⁰C. H. Brito Cruz, J. P. Gordon, P. C. Becker, R. L. Fork, and C. V. Shank, IEEE J. Quantum Electron. **QE-24**, 261 (1988).
- ³¹D. N. Batchelder and D. Bloor, J. Phys. C **15**, 3005 (1982).
- ³²B. Dick and R. M. Hochstrasser, Chem. Phys. **75**, 133 (1983).
- ³³B. Dick and R. M. Hochstrasser, J. Chem. Phys. **81**, 2897 (1984).
- ³⁴S. Saikan, N. Hashimoto, T. Kushida, and K. Namba, J. Chem. Phys. **82**, 5409 (1985).
- ³⁵K. Ichimura, M. Yoshizawa, H. Matsuda, S. Okada, M. Osugi, S. Hourai, H. Nakanishi, and T. Kobayashi, J. Chem. Phys. (to be published).